

## Insights from Modeling Three-Dimensional Structures of the Human Potassium and Sodium Channels

Kuo-Chen Chou\*

*Life Science Research Center, Shanghai Jiaotong University, Shanghai 200030, China,  
Tianjin Institute of Bioinformatics and Drug Discovery (TIBDD), Tianjin 300074, China,  
and Gordon Life Science Institute, 13784 Torrey Del Mar, San Diego, California*

Received March 29, 2004

Ion channels allow the movement of ions across cell membranes. Nearly all cells have membranes spanned by ion channels, without which human nerves simply would not work. Ion channels are formed by the aggregation of subunits into a cylindrical configuration that allows a pore, thus forming a kind of tube for ion trafficking. In the present study, the subunits of the human potassium channel are formed by four identical protein chains, whereas for the case of the human sodium channel, the corresponding subunits are actually four hetero-domains formed by the folding of a very large but single protein chain. Since both of the two ion channels are important targets for drug discovery, the 3D (dimensional) structures of their pore regions were developed. On the basis of the 3D models, some important molecular biological mechanisms were discussed that may stimulate novel strategies for therapeutic treatment of the diseases related to ion channel disorders, such as long QT syndrome and chronic pain.

**Keywords:** pore region • membrane-spanning protein • channel architecture • pore • selectivity filter • HERG • hPN3

### I. Introduction

Ion channels are found in every living thing. They span the cellular membrane, forming passage ways, or pores, through which ions flow down electrochemical gradients. Regulated by voltage, cyclic nucleotides, or neurotransmitters, these channels can conduct high-speed streams of potassium, sodium, calcium, and chloride ions into cells. Their hallmark features include discriminating selectivity, rapid-fire conduction rates, and gating. Owing to these features, it is vitally important to understand their 3D structures, and why they are so good at selectivity. Without such selectivity, living things would die.

It has long been known that the flows of potassium and sodium ions are affected by the changes in membrane action potentials, and that the ion channels have conduction, selection, and gating functions. But what do the channels look like? How do they conduct ions? How do metabolic cues regulate channel gating? These questions could not be seriously addressed until the structure of the ion channels in the atomic level was revealed. In 1998, the first crystal structure of the potassium channel, known as the KcsA channel, from the bacterium *Streptomyces lividans*, was reported.<sup>1</sup> Because both prokaryotic and eukaryotic pores are closely related, the channel's architectural design is essentially the same for higher organisms as well. On the basis of this, it is rational to use the crystal structure of KcsA as a template to model the human potassium and sodium channels, respectively, and discuss the insights thus obtained.

### II. Human Potassium Channel

The HERG (Human Ether-a-go-go-Related Gene) potassium channel is formed by four identical subunits, each having 1058 amino acid residues<sup>2</sup> folded into six transmembrane domains: S1, S2, S3, S4, S5, and S6. However, the core of the channel is formed by S6 domain as well as a pore helix preceding to it.<sup>1</sup> Accordingly, our attention can just focus on the region of res.612–669. Although the sequence position is slightly different with res.610–667 as defined by Mitcheson et al.,<sup>3</sup> the sequence itself in both cases is the same. Furthermore, the sequence position defined here is consistent with the information deposited into the data bank by Shoeb et al.<sup>2</sup> with the accession number: AAN05415. Because the potassium channel is a homotetramer (Figure 1a), the sequence alignment between HERG and KcsA needs to be done only for one of the four constituent subunits, and within the aforementioned region.

The sequence alignment was performed using the PILEUP program in the GCG package.<sup>4</sup> The result of the sequence alignment is given in Figure 1b, based on which as well as the atomic coordinates of KcsA (1b18.pdb), the 3D structure of HERG (1kcc) was developed. To avoid the occurrence of any conflicting structure with overlap or penetration among the constituent subunits, the microenvironment effects were taken into account during the model-building process, as done in modeling the GABA-A receptors.<sup>5</sup> During the above operation, each of the subunit chains was computed by using the segment matching modeling method, in which a database of known protein structures was employed to build an unknown target

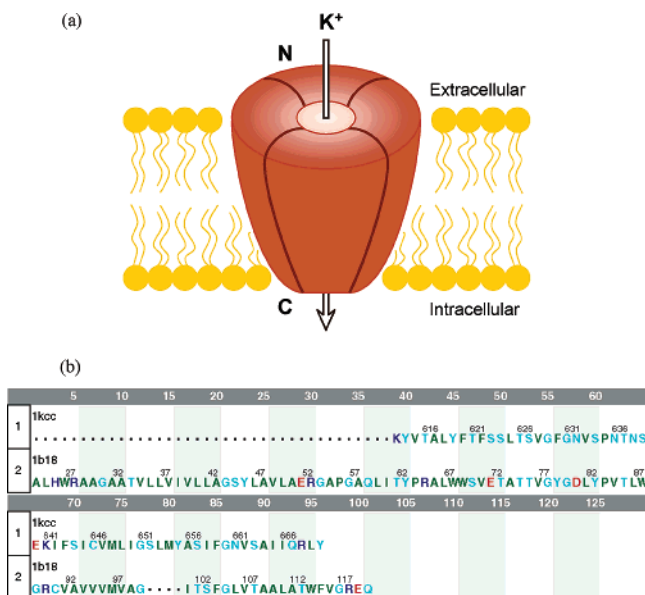


**Figure 1.** (a) Schematic drawing to show the membrane-spanning potassium channel consisting of four identical subunits. (b) Sequence alignment of HERG (1kcc) with KcsA (1b18) by using the PILEUP program in the GCG package (4), where hydrophobic amino acids are green, hydrophilic in light blue, acidic in red, and basic in dark blue.

structure based on an amino acid sequence alignment.<sup>6–10</sup> In the current case, the target structure was each of the subunits in a homotetramer that are to be predicted. The modeling consisted of the following procedures: (a) the target structure was first broken into short segments of sequence; (b) the database (formed by more than 5200 high-resolution X-ray protein structures) was searched for matching segments according to the sequence alignment and the shape of the template protein; (c) these segments coordinates were fitted into the growing target structure under the monitor to avoid any van der Waal overlap until all atomic coordinates of the target structure were obtained; and (d) the process was repeated 10 times and an average model was generated, followed by energy minimization of the entire chain with the presence of the corresponding other three chains as an environment. Finally, the four chains thus generated were subject to an overall energy minimization with respect to all the atoms to create the final 3D models for the HERG K<sup>+</sup> channel. The above segment matching approach was successfully used to model the protease domains of caspase-8<sup>11</sup> and caspase-9,<sup>12</sup> predict CARDs (CASPase Recruitment Domains) of Apaf-1, Ced-4, and Ced-3 based on the NMR structure of the RAIDD CARD,<sup>13</sup> as well as model the Cdk5-P35 complex.<sup>14</sup> Recently, the similar approach was also used to predict the tertiary structure of  $\beta$ -secretase zymogen<sup>15</sup> successfully elucidating the experimental observations that the prodomain of  $\beta$ -secretase does not suppress activity as in a strict zymogen.<sup>15</sup>

The 3D structure thus obtained for HERG channel is shown in Figure 2a, which has all of the typical features of potassium channels<sup>1</sup> as outlined below. Each subunit contains a short helix called “pore helix” (yellow) and a long helix called “inner helix” (light blue) with an insertion of a short loop (purple). Four inner helices converge together in a bundle, much like an inverted teepee, on the cell membrane’s intracellular side. The four outer helices facing the lipid membrane are not included since the HERG sequence for this part is outside the

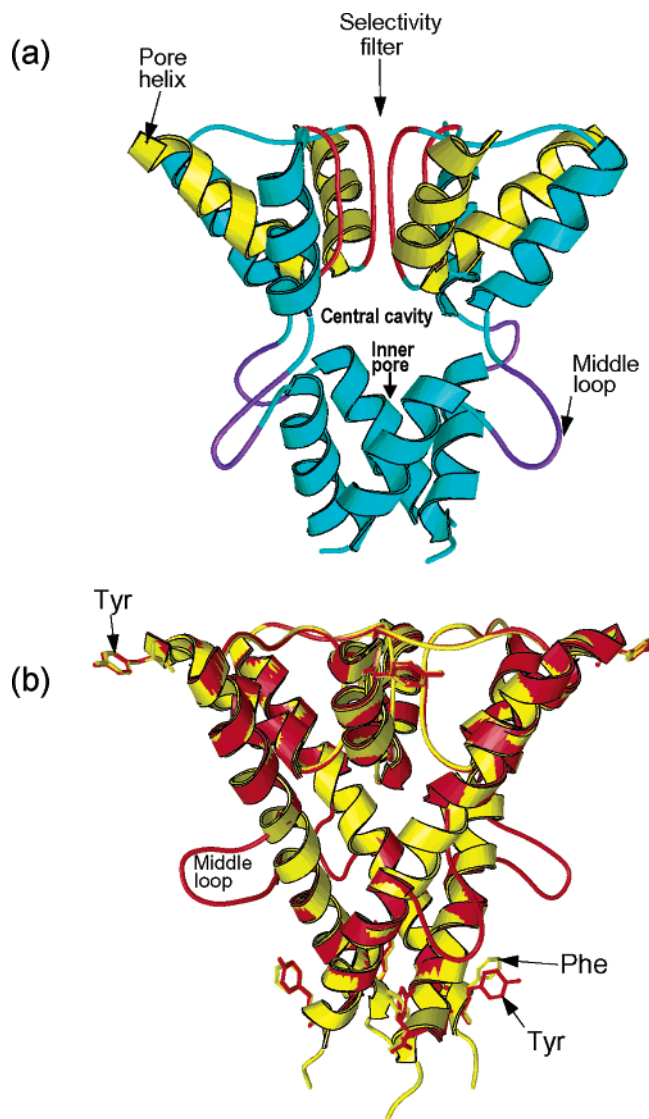


**Figure 2.** (a) Ribbon drawing of the predicted 3D structure of HERG channel, where the selectivity filter region is in red, the short pore helices in yellow, the inner helices in light blue, and the middle loops purple. (b) A superposition of the HERG channel (red) with the KcsA channel (yellow).

focus of the current study (see Figure 1b). Spanning the lipid membrane, the HERG K<sup>+</sup> channel is about 34 Å in length.

A superposition of the HERG channel with KcsA channel is given in Figure 2b, where KcsA is in yellow and HERG in red. As shown from the figure, a remarkable difference between the two pore proteins is as follows: the HERG channel has four middle loops but the KcsA channel does not. This is due to the existence of a segment insertion (res.651–654) in the HERG channel, as shown in Figure 1b. Such a difference may be related to the structural flexibility without affecting the function of the highly selective channel for K<sup>+</sup> ions, as will be further discussed below. One of the typical structural features for potassium channels is with aromatic amino acids on the membrane-facing surface at both extracellular and intracellular layers. On the extracellular layer, the aromatic amino acids are Tyr for both KcsA and HERG; but on the intracellular layer, they are Phe for KcsA while Tyr for HERG.

As shown in Figure 2a, the HERG potassium channel consists mainly of three regions:<sup>1</sup> selectivity filter,<sup>2</sup> central cavity, and<sup>3</sup>

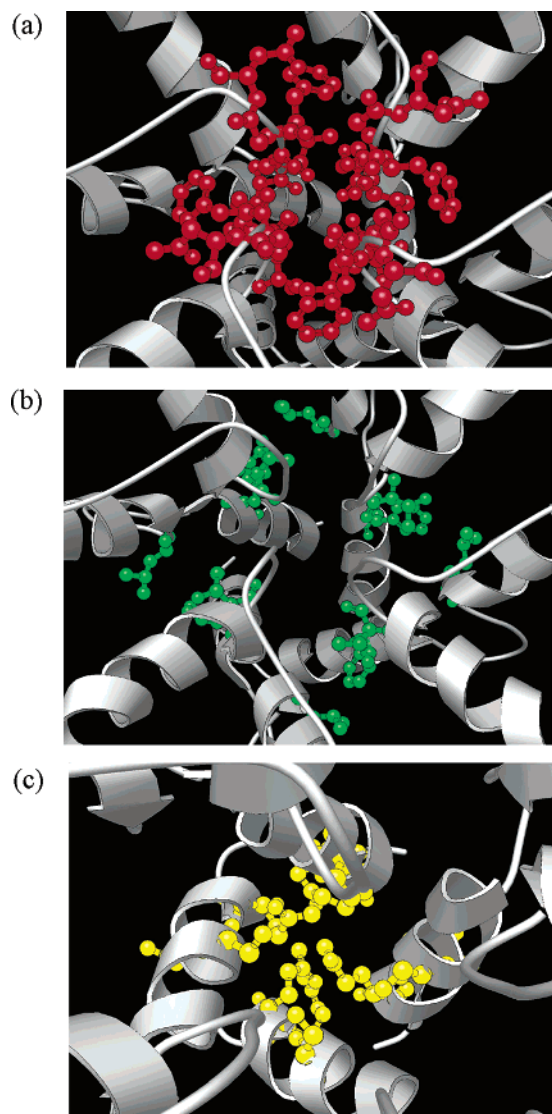


**Figure 3.** Snapshots taken right in front of (a) the selectivity filter, (b) the central cavity, and (c) the inner pore.

inner pore. Shown in Figure 3 are the snapshots taken right in front of (a) the selectivity filter, (b) the central cavity, and (c) the inner pore. As is well-known, the  $K^+$  channels exhibit 10 000-fold greater selection of potassium over sodium ions. The chemistry underlying how potassium ions flow through the channel, i.e., the mechanism of potassium hydration and dehydration, ion conduction, and the role of the selectivity filter, has been illustrated for the KcsA channel,<sup>16–18</sup> and can be similarly used to the HERG channel as well. The process of  $K^+$  ions passing through the HERG channel can be briefed as follows. (1) To pass through the channel, potassium ions have to first go through the selectivity filter by leaving their water-filled environment and entering into the selectivity filter (Figure 2a), which is lined with oxygen atoms from surrounding carbonyl groups (Figure 3a). These oxygen atoms mimic a water-filled environment. At this point, the filter discriminates, determining which ions are allowed to pass. The oxygen atoms cradle the potassium ions as snugly as the water molecules did; the cradle is a bit too large for the smaller sodium ions, which remain behind in the water environment where they are more stable. It is through the selectivity filter that the channel achieves both specificity and thermodynamically favorable

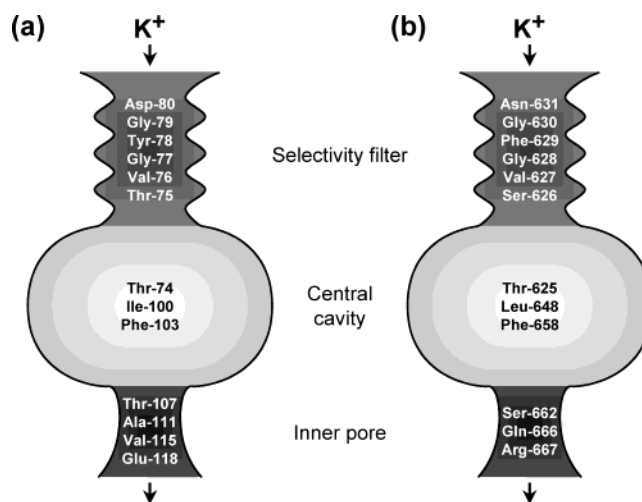


**Figure 4.** Key residues in the three regions of (a) the KcsA channel and (b) the HERG channel according to the order from top (extracellular) to the bottom (intracellular).

environment conducive to potassium ion flow<sup>16–18</sup>. (2) Subsequently, the potassium ions move into the central (Figure 2a) and wider cavity (Figure 3b), the so-called “inner vestibule” of the pore, retaining their hydration. (3) The last step, i.e., the process for potassium ions passing into cells through the inner pore (Figure 2a, Figure 3c), is related to an open-channel conformation, as revealed recently by the calcium-mediated gating mechanism of the potassium channel.<sup>19,20</sup> These authors found that the open conformation of the pore was surprisingly large. There is a conserved glycine residue, i.e., res.99 for KcsA and res.650 for HERG (see Figure 1b), located deep within the membrane, that functions as the gating hinge and permits the large conformational rearrangement. It is anticipated that the open-state structure is particularly feasible for the current model because the corresponding hinge-related residue in HERG channel, i.e., Gly-650, is followed by a loop (see Figure 1b and Figure 2a) that would make the local structure around it much more flexible, providing more room for conformational rearrangement. The above process allows  $K^+$  ions to pass the cell membrane with almost a diffusion-controlled rate<sup>21,22</sup> as if no barrier exists, but simultaneously acting as a concrete wall to the smaller  $Na^+$  ions. This is a vitally important biological function of  $K^+$  channels because living things would die without such selectivity.

The open-state structure revealed by the calcium-mediated gating mechanism is really intriguing; it is anticipated that many insights can be gained from it for the possible ways to pharmaceutically modulate the function of the channel. For facilitating comparison, the key residues in the three regions of (a) the KcsA channel and (b) the HERG channel are schematically listed in Figure 4 according to the order from top (extracellular) to the bottom (intracellular). As shown from the figure, the selectivity filter for KcsA is formed by the sequence TVGYGD, whereas that for HERG by the sequence SVGFNG, both containing four identical sequences from each of the four subunits. Since the sequence for the selectivity filter is highly conserved with only slight mutation, it is often called the “signature sequence” of the potassium channels. The central cavity of the KcsA channel is encompassed by four sets of Thr-74, Ile-100, and Phe-103, whereas that of the HERG channel by four sets of Thr-625, Leu-648, and Phe-658. The amino acids that form the inner pore have the least similarity



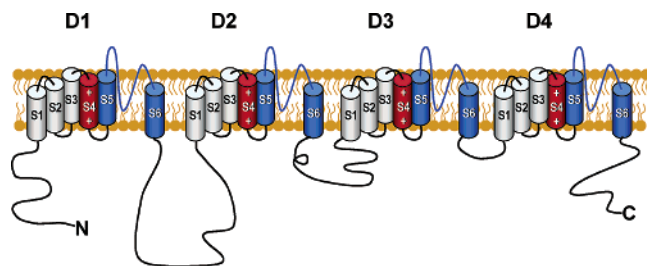


**Figure 5.** Schematic drawing of human tetrodotoxin-resistant voltage-gated sodium channel (hPN3). The trans-membrane protein consists of 1956 amino acids, roughly folded into four domains D1, D2, D3, and D4, each containing six trans-membrane segments S1, S2, S3, S4, S5, and S6. The core of sodium channel is formed by S5 and S6 (blue) from each of the four domains D1–D4.

between the KcsA channel and HERG channel. This is very likely due to the existence of the middle loops in the HERG channel (see Figure 2) that needs quite different residues in the inner pore to optimally modulate the conformational change for the open-state structure. The current findings might provide useful insights to drug design since the HERG channel is the major biological target by most of long QT syndrome inducing drug molecules.

### III. Human Sodium Channel

Voltage-gated tetrodotoxin (TTX)-resistant sodium channels present in primary sensory neurons may be responsible for the excitability of nociceptors, and may underlie pain and tenderness associated with tissue injury and inflammation. Use of nonselective sodium channel blockers as analgesics is limited by numerous adverse effects, such as nausea, emesis, dizziness, ataxia, cardiac effects, drowsiness, and blurred vision. These side effects are related to the lack of pharmacological selectivity. To develop drugs for chronic pain with high selectivity, the first important thing is to find the 3D structure of hPN3, i.e., human voltage-gated TTX-resistant sodium channel. The trans-membrane protein of hPN3 consists of 1956 amino acids,<sup>23</sup> and is roughly folded into four domains D1, D2, D3, and D4,<sup>24</sup> as shown in Figure 5. Each domain contains six trans-membrane segments S1, S2, S3, S4, S5, and S6.<sup>24</sup> It is known that the sodium channel is formed by S5/S6 from the four domains (D1 – D4) of PN3.<sup>24</sup> Cysteine mutagenesis and cross-linking experiments show that the loops between S5 and S6 of the four domains are in close proximity to each other,<sup>25</sup> and hence they are named P-loops (P means “pore”). Actually, when the four S5–P–S6 regions of a sodium channel were ligated together (so all the S1–S4 regions were missing), the structure thus formed would become an ionophore that conducted ions when activated by a sodium channel toxin,<sup>26</sup> although it did not reconstitute all aspects of a sodium channel. Accordingly, it is rational to use the four S5–P–S6 segments to build up the core of the sodium channel. To realize this, the sequence alignment of KcsA (potassium channel) with the four S5–P–S6 segments of hPN3 was conducted, as shown in Figure 6. Note that KcsA is a homo-tetramer, and hence only one chain is needed in the alignment. The sequences of S5–P–S6 in the four domains are different and hence we use PN3\_a, PN3\_b, PN3\_c, and PN3\_d to represent the four segments S5–P–S6 in domains D1, D2, D3, and D4, respectively. During the sequence alignment, the factor of hydrophobicity (Figure 6a and b) was taken into account as done in the heuristic approach.<sup>27</sup> Also, it is



**Figure 6.** Sequence alignment of KcsA (potassium channel) with the four S5/S6 segments of hPN3 that KcsA. Since KcsA is a homo-tetramer, only one chain is need in the alignment. The sequences of S5 and S6 in the four domains are different. We use (a) PN3\_1a, PN3\_1b, PN3\_1c, PN3\_1d to represent the four S5 segments in domains D1, D2, D3, D4, and (b) PN3\_2a, PN3\_2b, PN3\_2c, PN3\_2d to represent the corresponding four S6 segments, respectively, where hydrophobic amino acids are green, hydrophilic in light blue, acidic in red, and basic in dark blue. See text for further explanation.

known that Asp-356, Glu-849, Lys-1367, and Ala-1661 of hPN3, the so-called DEKA group, are involved in sodium selectivity<sup>28</sup> and located at the bottom of the selectivity filter.<sup>29</sup> Therefore, according to the knowledge-based modeling approach<sup>30</sup> their position in the sequence alignment should be located at the same position as Thr-118 of KcsA (Figure 6b).

On the basis of such a sequence alignment as well as the template of KcsA (1b18b.pdb), the 3D structure of the core channel of hPN3 was developed by the segment matching modeling procedures as described in Section II. Shown in Figure 7 is the ribbon drawing of the predicted structure. For facilitating comparison, a close view of the selectivity filters of the potassium channel and sodium channel are shown in Figure 8a and b, respectively. As we can see, the selectivity filters in both channels are lined with oxygen atoms from surrounding carbonyl groups. These oxygen atoms mimic a water-filled environment. At this point, the filter discriminates, determining which ions are allowed to pass. The potassium pore defined by the oxygen atoms is about 4.7 Å (Figure 8a), whereas the sodium pore is reduced to about 3.3 Å (Figure 8b) due to different microenvironment (such as the existence of Trp-1369). The van der Waals diameter of potassium ions is about 4 Å, and that of sodium ions 3.2 Å. These numbers indicate that the oxygen atoms in the potassium channel filter can provide a snug microenvironment to cradle the potassium ions. But the cradle is a bit too large for the smaller sodium ions, which remain behind in the water environment where they are more stable. In contrast, the sodium channel filter is a bit too narrow to allow potassium ions to pass through, but

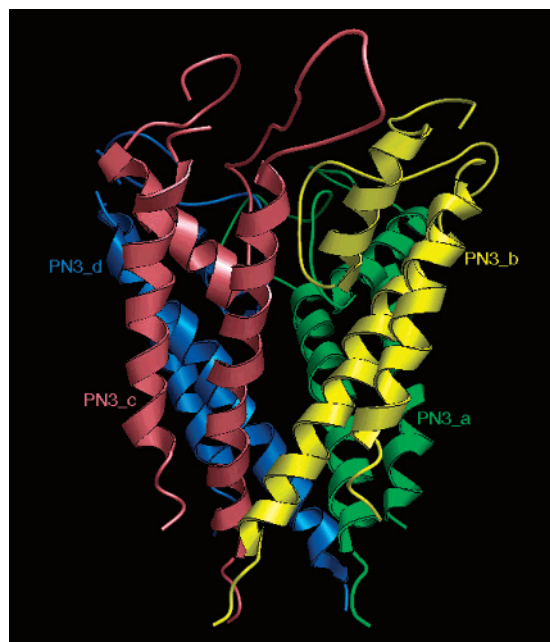


**Figure 7.** Ribbon drawing of the computed 3D core structure for the sodium channel of hPN3, where S5/S6 segments from domains 1–4 (D1–D4) are colored in green, yellow, magenta, and blue, respectively. Viewed perpendicular to the channel from extracellular (top) to intracellular (bottom).

is just right for cradling sodium ions, allowing them to pass through. The predicted 3D structure might provide some insight for understanding the molecular mechanism why hPN3 conducts only sodium ions, whereas KcsA only potassium ions. The current 3D structure may also serve as a footing for conducting mutagenesis and docking studies, stimulating novel strategies for the treatment of chronic pain with less adverse effects.

#### IV. Conclusion

Ions trafficking through the cell membrane of neurons determine their ability to signal and respond to each other. Because the cell membrane is almost totally impermeable to ions, there is a need to use specialized cellular devices, called “ion channels”, that can transport ions in and out of the cell through the membrane. Ion channels are formed of glycoproteins (proteins with sugar molecules attached) that traverse the cell membrane. There are about tens of different types of ion channels. In this study, we are focused on the HERG potassium channel and hPN3 sodium channel because they are currently important targets for drug discovery. The former is formed by four identical protein chains, whereas the latter by the folding of a single large protein chain into four hetero-domains. To develop the 3D structures of the two ion channels, in addition to the general homology approach, the heuristic approach<sup>27</sup> and knowledge-based approach<sup>30</sup> were used as well. Although computer-predicted protein structures are still not as accurate as X-ray structures, modeled structures such as the two presented here can be used to understand and test hypotheses about biological function. Particularly, the present models provide useful insights for understanding the mechanism why the sodium channel conducts only sodium ions, while the potassium channel conducts only potassium ions. The models can also serve as a structural frame for conducting mutagenesis

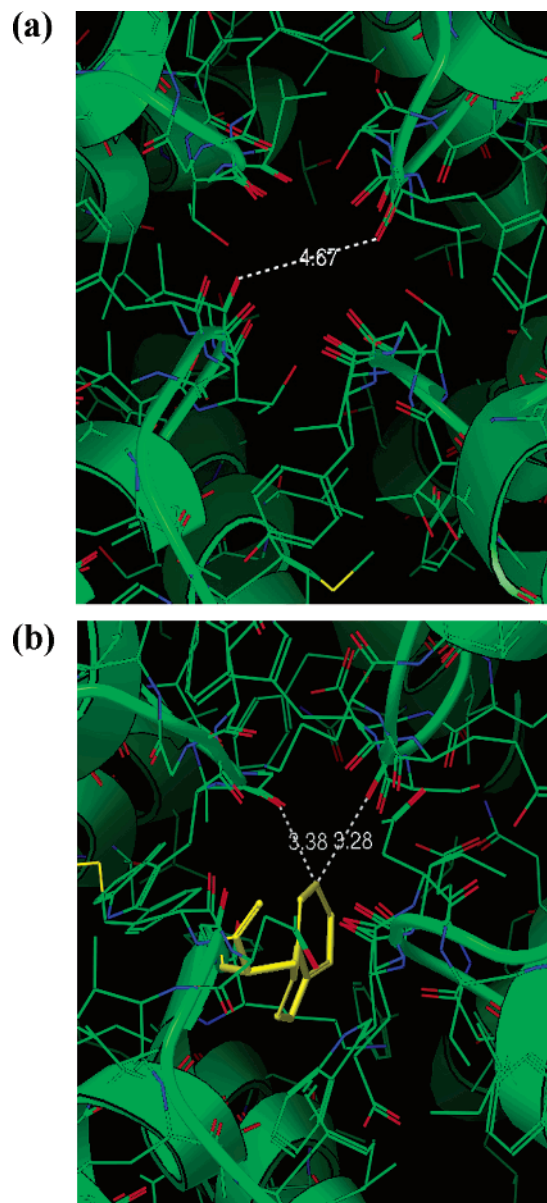


**Figure 8.** Close view of the selectivity filters of (a) the potassium channel and (b) the sodium channel. Both are lined with oxygen atoms (red) from surrounding carbonyl groups. These oxygen atoms mimic a water-filled environment. The pore defined by such lined-up oxygen atoms for the potassium channel is about 4.7 Å (panel a); whereas the corresponding pore for the sodium channel is reduced to about 3.3 Å (panel b) due to the side chain of Trp-1369.

and docking studies or as a footing for encouraging novel strategies in developing new drugs to treat ion channel disorders.

**Acknowledgment.** The author wishes to thank the two anonymous knowledgeable reviewers whose comments are very helpful in strengthening the presentation of this study.

#### References

- (1) Doyle, D. A.; Morais, C. J.; Pfuetzner, R. A.; Kuo, A.; Gulbis, J. M.; Cohen, S. L.; Chait, B. T.; MacKinnon, R. *Science* **1998**, *280*, 69–77.
- (2) Shoeb, F.; Malykhina, A. P.; Akbarali, H. I. **2002**, Unpublished results.

- (3) Mitcheson, J. S.; Chen, J.; Lin, M.; Culbertson, C.; Sanguinetti, M. C. *Proc. Natl. Acad. Sci. U.S.A.* **2000**, *97*, 12 329–12 333.
- (4) Devereux, J. In Genetic Computer Group (GCG), 1994, Madison, Wisconsin.
- (5) Chou, K. C. *Biochem. Biophys. Res. Commun.* **2004**, *316*, 636–642.
- (6) Jones, T. A.; Thirup, S. *EMBO J.* **1986**, *5*, 819–822.
- (7) Blundell, T. L.; Sibanda, B. L.; Sternberg, M. J. E.; Thornton, J. M. *Nature (London)* **1987**, *326*, 347–352.
- (8) Finzel, B. C.; Kimatian, S.; Ohlendorf, D. H.; Wendoloski, J. J.; Levitt, M.; Salemme, F. R. In *Crystallographic and Modeling Methods in Molecular Design*; Bugg, C. E., Ealick, S. E., Eds.; Springer-Verlag: Berlin, 1989; pp 175–188.
- (9) Levitt, M. *J. Mol. Biol.* **1992**, *226*, 507–533.
- (10) Chou, K. C.; Nemethy, G.; Pottle, M.; Scheraga, H. A. *J. Mol. Biol.* **1989**, *205*, 241–249.
- (11) Chou, K. C.; Jones, D.; Heinrikson, R. L. *FEBS Lett.* **1997**, *419*, 49–54.
- (12) Chou, K. C.; Tomasselli, A. G.; Heinrikson, R. L. *FEBS Lett.* **2000**, *470*, 249–256.
- (13) Chou, J. J.; Matsuo, H.; Duan, H.; Wagner, G. *Cell* **1998**, *94*, 171–180.
- (14) Chou, K. C.; Watenpaugh, K. D.; Heinrikson, R. L. *Biochem. Biophys. Res. Commun.* **1999**, *259*, 420–428.
- (15) Chou, K. C.; Howe, W. J. *Biochem. Biophys. Res. Commun.* **2002**, *292*, 702–708.
- (16) Zhou, Y.; J. H.; M.-C.; Kaufman, A.; MacKinnon, R. *Nature* **2001**, *414*, 43–48.
- (17) Morais-Cabral, J. H.; Zhou, Y.; MacKinnon, R. *Nature* **2001**, *414*, 37–42.
- (18) Miller, C. *Nature* **2001**, *414*, 23–24.
- (19) Jiang, Y.; Lee, A.; Chen, J.; Cadene, M.; Chait, B. T.; MacKinnon, R. *Nature* **2002**, *417*, 523–526.
- (20) Jiang, Y.; Lee, A.; Chen, J.; Cadene, M.; Chait, B. T.; MacKinnon, R. *Nature* **2002**, *417*, 515–522.
- (21) Chou, K. C.; Jiang, S. P. *Sci. Sinica* **1974**, *17*, 664–680.
- (22) Chou, K. C. *Sci. Sinica* **1976**, *19*, 505–528.
- (23) Rabert, D. K.; Koch, B. D.; Ilnicka, M.; Obornolte, R. A.; Naylor, S. L.; Herman, R. C.; Eglen, R. M.; Hunter, J. C.; Sangameswaran, L. *Pain* **1998**, *78*, 107–114.
- (24) Catterall, W. A. *Neuron* **2000**, *26*, 13–25.
- (25) Benitah, J. P.; Chen, Z. H.; Balsler, J. R.; Tomaselli, G. F.; Marban, E. *J. Neurosci.* **1999**, *19*, 1577–1585.
- (26) Chen, Z.; Alcayaga, C.; Suarez-Isla, B. A.; O'Rourke, B.; Tomaselli, G.; Marban, E. A. *J. Biol. Chem.* **2002**, *277*, 24653–24658.
- (27) Caracci, L.; Chou, K. C.; Maggiora, G. M. *Biochemistry* **1991**, *30*, 4389–4398.
- (28) Heinemann, S. H.; Terlau, H.; Stuhmer, W.; Imoto, K.; Numa, S. *Nature* **1992**, *356*, 441–443.
- (29) Yamagishi, T.; Janecki, M.; Marban, E.; Tomaselli, G. F. *Biophys. J.* **1997**, *73*, 195–204.
- (30) Chou, K. C. *J. Protein Chem.* **1996**, *15*, 161–168.

PR049931Q